Effect of surfactants on liquid side mass transfer coefficients: A new insight

Gilles Hebrard, Jikun Zeng, Karine Loubière

EFFECT OF SURFACTANTS ON LIQUID SIDE MASS TRANSFER COEFFICIENTS: A NEW INSIGHT

Gilles HEBRARD[1*], Jikun ZENG[1], Karine LOUBIERE[2]

1 *Laboratoire d'Ingénierie des Systèmes Biologiques et des Procédés (LISBP) UMR CNRS 5504 - INRA 792*
Institut National des Sciences Appliquées de Toulouse, 135 Avenue de Rangueil, 31077 Toulouse Cedex 4, France

2 *Laboratoire GEnie des Procédés-Environnement-Agroalimentaire (GEPEA) UMR CNRS 6144*
CRTT, Boulevard de l'Université, BP 406, 44602 Saint-Nazaire Cedex, France

* Corresponding author:
Gilles.Hebrard@insa-toulouse.fr; *Tel*: +33(0)5 61 55 97 89; *Fax*: +33(0)5 61 55 97 60 (G. Hebrard)

Abstract

Specific experiments are proposed to investigate the effect of surfactants on liquid side mass transfer coefficients. They are based on the determination of the liquid side mass transfer coefficient k_L at a free gas-liquid interface, under controlled temperature and hydrodynamic conditions. Firstly, the methodology is validated in water at various rotation speeds and temperatures. In a second time, it is applied in aqueous and pure solutions of anionic surfactants: a decrease of k_L with an increase of surfactant concentrations is then observed until leveling off when the *CMC* is reached. Deduced from experimental results, the equivalent diffusion coefficients describe an identical behavior. These results demonstrate that the lowest k_L are directly linked to the presence of surfactants at the gas-liquid interface which makes the diffusion coefficients of oxygen be reduced. At last, a comparison is performed with the data of [1-2] obtained from a chain of bubbles having diameters above to 3.5 mm. A quasi-linear relation between the k_L issued from both hydrodynamic configurations is revealed in the whole range of surfactant concentrations. Such findings would prove that, in both cases, the impact of surfactants on liquid side mass transfer coefficient is correlated with the changes in the diffusion coefficients of oxygen.

1. Introduction

Gas-liquid mass transfer is the object of an active research, actually focused on the understanding of the elementary mechanisms involved and of their complex interactions. In aerated reactor, one of the main bottlenecks deals with the effect of surfactants at the gas-liquid interface. Even if the approach based on Langmuir isotherm is commonly used to describe the bubble surface area covered by surfactants, it remains insufficient to well explain how the presence of surfactants at the gas-liquid interface can influence the mass

transfer efficiency. Many recent articles [1-10] have been published on this topic and thus give evidence that the effect of surfactants is still under debate. According to [3, 9-10], the presence of surfactants would induce a local modification of the slip velocity at the interface, responsible for the decrease of liquid side mass transfer coefficients. Some authors have suggested other explanations:

- surfactants would create both a modification of the local hydrodynamic at the interface and a new resistance to mass transfer due to a change in local diffusion at the boundary layer film [1-2];
- by reducing surface tension, the accumulation of surfactants at the interface would decrease interfacial renewal and so the diffusion of gas into the liquid [6].

This paper attempts to get a new insight into the understanding of this phenomenon by means of specific experiments. For that, the liquid side mass transfer coefficient k_L at a free gas-liquid interface will be determined under controlled hydrodynamic conditions, at various temperatures and for different surfactant concentrations. Thanks to the knowledge of both interfacial velocity and interfacial area involved, the diffusion coefficient of oxygen will be then deduced. At last, these results, obtained at a free gas-liquid interface, will be compared with the ones measured by [1-2] at gas-liquid interfaces formed by a chain of bubbles (having diameters above to 3.5 mm).

The present communication is composed of two parts: the first one is devoted to the material and methods, and the second to the results and comments related to the effects of surfactants at gas-liquid interfaces.

2. Material and Methods

2.1. *Experimental device*

Schematically represented in Figure 1, the experimental device enables the volumetric mass transfer coefficient, k_La, occurring at a free gas-liquid interface to be determined under controlled hydrodynamic conditions. It consists of a double wall glass vessel, 0.065 m in internal diameter and tightly closed. The vessel is filled with a 0.035 m height of liquid (H_L). A magnetic agitator enables bulk agitation of liquid without appreciable wave motion. The free surface remains flat in the whole range of rotation speeds used in the experiments (N = 50 - 120 rpm). The rotation speed is kept very small so as to maintain a constant surface of the gas-liquid interface offered to the mass transfer whatever the experiments. The temperature's control is ensured by a liquid circulation through the vessel's jacket associated to a thermo-regulated system. The temperature in the cell is measured by means of a thermometer. The experiments are carried out batch wise with respect to the liquid- and continuous to the gas-phase. Gas is fed above the liquid surface (connection through the cell's cap) and is controlled by a gas flow meter. A gas flow rate of $2.85.10^{-6}$ $m^3.s^{-1}$ is fixed whatever the experiments: this low value hinders any surface deformation and enables a constant interfacial shear stress to be imposed. A three-way valve is used to inject either air or nitrogen (atmosphere flushing).

2.2 *Gas and liquid phases*

Compressed air and nitrogen from laboratory lines are the gas phases. It is particularly important to clean them to avoid any unwanted contamination (such as solid particles or organic substances) in the gas-liquid systems under test. For that, both particle-retention and activated-carbon filtering are used.

Three kinds of liquid phases are used: water, aqueous solutions of surfactant and pure solution of surfactant.

Water comes from an ion exchanger and is treated by activated- carbon filtering. At 20°C, the conductivity of water is 0.2 µS.cm^{-1} (WTW® Conductivity Meter LF538), the Total Organic Carbon is 0.216 ppm (Shimadzu® TOC-VCSH analyzer) and the pH is 7.3 (WTW® Microprocessor pH Meter pH539). For different temperatures varying between 5 and 50°C, density and dynamic viscosity of water are measured by means of a pycnometer and a viscometer (RM180 Rheomat Rheometric Scientific®) respectively. Their values are reported in Table 1.

As in [1-2], the surface active agent used is an anionic surfactant, commercially known as Texapon® and mainly composed of sodium laurylsulfate (molecular weight of 382 g.mol^{-1}). It is the most used surfactant for fabrication of soaps, detergents or emulsifying agents, and thus the most frequently present in wastewaters. The aqueous solutions of surfactants are prepared with the water previously described. Various concentrations are tested, ranging between 0.05 and 10 g.L^{-1}. As for water, their densities and dynamic viscosities are measured: for all solutions, no significant differences with water are found at T = 20°C (Table 2). This result is not surprising with regard to the small values of concentrations tested. According to [1-2], this surfactant is characterized by a Critical Micelle Concentration of 1.9 g.L^{-1}, a surface concentration at saturation Γ_∞ of 6.52.10^{-6} mol.m^{-2} and an adsorption constant at equilibrium K of 6.25 m^3.mol^{-1}. In Table 2 are also reported, for each aqueous solution, the static surface tension σ_L (Digidrop GBX® and Krüss® tensiometers) and the surface coverage ratio at equilibrium s_e. In addition, it is interesting to note that the diffusion kinetics of this surfactant at gas-liquid interfaces is fast: dynamic surface tension measurements have shown that the time necessary to reach the static surface tension is close to 0.2 s [11]. This time is significantly smaller than the characteristic times

of mass transfer $1/k_L a$ here measured (Tables 1 and 3). This is a relevant point for this study.

At last, a pure solution of surfactant is tested. The associated properties are reported in Table 2.

Note that: (i) all the experiments are run between three and six times, (ii) in presence of surfactants, the temperature is kept at 20°C, and (iii) before each experiment, a great care is taken for cleaning the experimental device in order to remove any trace of surfactant.

2.3 *Methods*

The experiments run are based on the experimental determination of the liquid mass transfer coefficient occurring at a free gas-liquid interface (device aforementioned) and, by considering a theoretical development, on the calculation of the diffusion coefficient of oxygen.

2.3.1 Gas-liquid mass transfer coefficient measurements

The well-known dynamic gassing-in and gassing-out method is used to determine the volumetric mass transfer coefficient $k_L a$. It is based on an oxygen mass balance in the liquid phase under unsteady-state condition. As the liquid phase is perfectly mixed and no chemical reaction is in presence, it is written as:

$$k_L a.(C^* - C) = \frac{\mathrm{d}C}{\mathrm{d}t} \tag{1}$$

where C^* is the dissolved oxygen concentration at saturation. When integrated, Eq. (1) becomes:

$$\mathrm{Ln}\frac{C^* - C}{C^* - C_0} = -k_L a \cdot t \tag{2}$$

where C_O is the dissolved oxygen concentration at the initial time.

The time-variation of the dissolved oxygen concentration, C, is measured by means of an Unisense® micro-probe (type OX 25-4046) and an acquisition system connected to a computer. Figure 2 presents an example of response curve, in where the signal S emitted by the probe is reported versus time. This signal is related to the dissolved oxygen concentration C as follows:

$$C = \alpha \cdot \frac{S - S_0}{S^* - S_0} \tag{3}$$

where α is the solubility of the oxygen into the liquid phase. The combination of Eqs. (2) and (3) leads to:

$$\mathrm{Ln}\frac{S^* - S}{S^* - S_0} = -k_L a \cdot t \tag{4}$$

At last, the $k_L a$ value is determined from the slope of the curve defined by Eq. (4), as illustrated in Figure 3. The response time of the Unisense® micro-probe is equal to 0.5 s and is very short when compared to the experiment duration (10^2-10^4 s): no correction is then necessary.

For each experiment, the following procedure is applied. At the beginning, the liquid phase is introduced inside the well-cleaned vessel (H_L = 0.035 m) and mixed with a small rotation speed (N = 100 rpm). When the thermal steady state is reached, nitrogen is injected until the dissolved oxygen concentration is reduced close to zero. Afterwards, nitrogen is replaced by air and the time-variation of the dissolved oxygen concentration is then recorded until saturation (Figure 2).

Whatever the experiments, the free surface is kept flat by applying both slow agitation rate and gas flow rate. The surface area offered to gas-liquid mass transfer can thus be reasonably assumed equal to the liquid surface S_L (i.e. to the horizontal section area of the vessel). The interfacial area a is then calculated by:

$$a = \frac{S_L}{V_L} \tag{5}$$

where V_L is the liquid volume. At last, a is equal to 28.57 m^{-1}.

The liquid side mass transfer coefficient k_L is then deduced from:

$$k_L = \frac{k_L a}{a} \tag{6}$$

2.3.2 Determination of the oxygen diffusion coefficient

In the experiments run, a gas flow (Q_G = 2.85.10^{-6} $m^3.s^{-1}$) is moving at a constant velocity U_G above a liquid phase which velocity (U_L) remain very low (the liquid surface being kept flat thanks to N = 100 rpm). In such conditions, the gas-liquid mass transfer is mainly controlled by the level of turbulence imposed by the gas flow above the interface [12]. The interfacial momentum transfer stress τ_i is then expressed as:

$$\tau_i = \frac{1}{2}.\rho_G.f_i.(U_G - U_L)^2 \tag{7}$$

where f_i is the interfacial friction factor. The interfacial momentum transfer velocity is then defined by:

$$U_i^* = \sqrt{\frac{\tau_i}{\rho_L}} \tag{8}$$

Danckwerts [13] proposed a modelling of the liquid side mass transfer coefficient based on the renewal rate of liquid elements at the gas-liquid interface *s'* with respect to:

$$k_L = \sqrt{D \times s'} \tag{9}$$

where D the diffusion coefficient of the solute in the liquid phase. Fortescue and Pearson [14] expressed this latter parameter for a free interface sheared by a gas flow as

$$s' = C_3 \times \varepsilon \tag{10}$$

where C_3 is a constant and ε the ratio between the characteristic scales of velocity and length. The interfacial shear stress is linked to the viscosity by the following equation:

$$\mu_L = \frac{\tau_i}{\varepsilon} \tag{11}$$

By combining Eqs (9-11), the liquid side mass transfer coefficient can be expressed as:

$$k_L = \sqrt{D.C_3.\frac{\tau_i}{\mu_L}} \tag{12}$$

By introducing the Schmidt number *Sc* in Eqs. (8) and (12), the Danckwerts model becomes:

$$\frac{k_L}{U_i^*}.Sc^{0.5} = C_1 \tag{13}$$

This is the general form of correlations related to absorption coefficients. In fact, the power of the Schmidt number depends on the nature of interfaces: for solid boundaries, it is equal to $^2/_3$ instead of ½ in the present case. Banerjee [15] proposed a constant C_1 varying between 0.108 and 0.158 in the case of sheared gas-liquid stratified interfaces. Cockx et al [16] unified data in horizontal stratified flows and in vertical bubbly flows with respect to C_1 = 0.1 ± 0.02.

In the experiments run, both low gas flow and agitation rates are always imposed. It can be then reasonably assumed that the interfacial momentum transfer stress τ_i, and thus the associated velocity U_i^*, remains constant for similar phase properties. In such conditions, the diffusion coefficient D in the liquid phase is expressed as:

$$D = \frac{\mu_L}{\rho_L}\left(\frac{k_L}{C_1 \cdot U_i^*}\right)^2 = \frac{\mu_L}{\rho_L}\left(\frac{k_L}{C_2}\right)^2 \tag{14}$$

where the constant C_2 is defined by the product between the constant C_1 and the interfacial momentum transfer velocity U_i^*.

Knowing the liquid mass transfer coefficient k_L (k_La measurements and Eq. 6) and the liquid phase properties (Tables 1-2), the diffusion coefficient of oxygen in the liquid phases under test will be easily deduced from Eq. (14). In addition, specific experiments will be carried out to determine the constant C_2 and to validate the assumptions linked to Eq. (14) with regard to the present experimental device (see below).

2.3.3 Empirical correlations for estimating diffusion coefficients

The diffusion coefficients deduced from the present methodology will be compared with the estimations issued from several correlations. Many correlations are available in the literature for diffusion coefficients in the liquid phase. Most are restricted to binary diffusion at infinite dilution, D_{AB}^{0}, or to self-diffusivity, reflecting thus the complexity of liquids on a molecular level (volumetric and thermodynamic effects due to composition variations). Note that, for concentrations greater than a few mole percent of A (solute) and B (solvent), these correlations have to be imperatively corrected to obtain the true diffusivity. Many authors strongly advice to prefer diffusivity data available at the conditions of interest over the predictions of any correlations [17]. For oxygen in water, the following data are found for example:

- at T = 20°C, $D = 1.8.10^{-9}$ m^2.s^{-1} [18],
- at T = 20°C, $D = 2.1.10^{-9}$ m^2.s^{-1} [12],
- at T = 25°C, $D = 2.5.10^{-9}$ m^2.s^{-1} with an estimated error of 20% [17]; using a constant ratio $D.\mu / T$ leads to $D \approx 2.2.10^{-9}$ m^2.s^{-1} at T = 20°C,
- at T = 25 °C, $D = 2.41.10^{-9}$ m^2.s^{-1} [19]; by using the previous temperature-correction, D is found equal to $2.13.10^{-9}$ m^2.s^{-1} at T = 20°C.

With regard to the previous values, the following average value will be assumed at T = 20°C for the determination of the constant C_2,

$$D = 2.10^{-9}\ \mathrm{m}^2.\mathrm{s}^{-1} \quad (15)$$

For general mixtures of dilute binary nonelectrolytes, the Wilke-Chang correlation [20] for D_{AB}^0 is one of the most widely used. It is an empirical modification of the Stokes-Einstein equation. It is not very accurate, however, for water as the solute; otherwise, it applies to diffusion of very dilute A in B. The associated average absolute error has been estimated, for 251 different systems, to 10% [17]. The Wilke-Chang correlation is expressed as:

$$D_{AB}^{o} = 7.4 \cdot 10^{-12} \frac{(\phi_B \cdot M_B)^{0.5} \cdot T}{\mu_B \cdot V_A^{\ 0.6}} \quad (16)$$

where M_B is the molecular weight of solvent (18.015 g.mol^{-1} for water), T is temperature (°K), μ_B is the solvent viscosity (cP) and V_A is the molar volume of the liquid solute at its normal boiling point (cm^3.mol^{-1}). The latter parameter is obtained from a group contribution approach: for oxygen, V_A is taken either as 28.02 cm^3.mol^{-1} [12] or as 25.6 cm^3.mol^{-1} [21]. ϕ_B is an association factor of solvent B: it was originally stated as 2.6 for water [20], but an empirical best fit with a value of 2.26 was found after reanalyzing the original data [21].

The Scheibel correlation [22] is also valid for general mixtures of dilute binary nonelectrolytes. It is established from a modification of the Wilke-Chang correlation where the association factor ϕ_B is eliminated:

$$D_{AB}^{0} = \frac{8.2 \cdot 10^{-12} \cdot T}{\mu_B \cdot V_A^{\ 1/3}} \left[1 + \left(\frac{3V_B}{V_A} \right)^{2/3} \right] \quad (17)$$

where V_B is the molar volume of solvent at normal boiling point (cm^3.mol^{-1}), all the others symbols have the same meaning as in Eq. 16. V_B is also estimated by a group contribution scheme. For water, a value of 18.1 cm^3.mol^{-1} is commonly accepted [12].

Hayduk and Laudie [23] presented a simple correlation for the infinite dilution diffusion coefficients of nonelectolytes in water. It is about the same accuracy (5.9%) as the Wilke-

Chang correlation. There is no explicit temperature dependence, but the 1.14 exponent on μ_B compensates for the absence of T in the numerator. This correlation is given by:

$$D_{AB}^{0} = \frac{13.26.10^{-9}}{\mu_B^{1.14}.V_A^{0.589}} \quad (18)$$

where all symbols have the same meaning as in the previous equations.

Other correlations in binary liquids, such as the Reddy-Doraiswamy [24], the Lusis-Ratcliff [25], the Tyn-Calus [26], the Umesi-Danner [27], the Siddiqi-Lucas [28] correlations, are also available but less useful and/or adapted. The comparison with the measured diffusion coefficients will be then limited to the three correlations related to Eqs. (16-18).

3. Results and discussion

Firstly, the method implemented will be validated by specific experiments. Afterwards, the application in presence of surfactants will be presented and discussed.

3.1 *Validation of the method*

Firstly, the constant C_2 has to be defined for deducing the diffusion coefficient from Eq. (14). One possible calibration is to consider the case of oxygen diffusion in water at 20°C insofar as the associated coefficient is well-referenced (see above). Six measurements were run to access the liquid side mass transfer coefficient k_L in this condition: they lead to k_L = $9.91.10^{-6}$ ± $0.95.10^{-6}$ $m.s^{-1}$ (Table 1). The combination of these data with Eqs. (14-15) converges toward:

$$C_2 = 2.22.10^{-4} \pm 0.21.10^{-4}\ \mathrm{m.s^{-1}} \quad (19)$$

To evaluate the accuracy of the latter constant, the experiments are reproduced for the same conditions (oxygen, water) but for different temperatures (5, 35 and 50°C). The averaged values of the coefficients k_L measured are reported in Table 1. They are used to calculate the associated diffusion coefficients D according to Eqs. (14, 19). For the same temperatures, the

diffusion coefficients of oxygen in water are also estimated by the Wilke-Chang (Eq. 16), Scheibel (Eq. 17) and Hayduk-Laudie (Eq. 18) correlations. The results are regrouped in Figure 4, dependently if the molar volume of oxygen V_A is taken equal to 25.2 or to 28.02 $cm^3.mol^{-1}$. Whatever the correlations and temperatures, the measured diffusion coefficients are in agreement with the estimated ones: the relative deviation never exceeds 10%. This result demonstrates that the value of the constant C_2 given in Eq. 19 is valid. This is coherent insofar as, whatever the temperatures, the same hydrodynamics conditions (gas flow rate and magnetic agitation) are applied, conserving thus the slip velocity. This implies that the interfacial momentum transfer stress τ_i remains constant (Eq. 7) and also the associated velocity U_i^* (Eq. 8) as the changes in water densities are not significant (Table 1), and even if the changes in water viscosities are important.

The constant C_2 is defined by the product between the constant C_1 and the interfacial momentum transfer velocity U_i^* (Eq. 14). By taking, in first approximation, a constant C_1 of 0.1 [16], U_i^* is found close to 2.10^{-3} $m.s^{-1}$. From this, an order of magnitude of the mass boundary layer δ_M can be obtained according to [29]:

$$\frac{\delta_M}{\delta} = Sc^{-1/3} \tag{20}$$

where δ is the hydrodynamic boundary layer approximate to

$$\delta = \frac{26\mu_L}{\rho_L.U_i^*} \tag{21}$$

At last, δ_M is found close to 1.5 mm. This low value tends to demonstrate that, at the liquid side interface, mass transfer is controlled rather by the shear imposed by the gas flow than by the liquid motion.

To get definitive confirmation, specific experiments are run in the same previous conditions (oxygen, water, 20 °C, Q_G = 2.85.10^{-6} m^3.s^{-1}) but for different rotation speeds N varying between 50 and 120 rpm. The mass transfer coefficients k_L measured are reported in Table 3 as well as the constant C_2 deduced from these values and Eqs. (14-15). When taking into account the experimental uncertainties (about 10%), no significant effect of the rotation speeds on the constant C_2 is observed, except for the highest N (120 rpm) where a slight decrease in C_2 appears. These data coupled with the previous findings confirm that the approach implemented for determining diffusion coefficients is relevant if the rotation speed does not exceed 100 rpm.

3.2 *Effect of surfactants on liquid side mass transfer coefficient*

The variation of liquid side mass transfer coefficients is presented as a function of surfactant concentration in Figure 5. It can be observed that k_L decreases with an increase of the surfactant concentration. A plateau is reached when the surfactant concentration is equal to the Critical Micellar Concentration *CMC* (1.9 g.L^{-1} at 20 °C, [1]), or in others words when the surface coverage ratio at equilibrium, s_e, becomes equal to one (Table 2). For higher concentrations, as the interface is totally covered by surfactants, any change in k_L is obtained. In Figure 5 (dashed line) is also reported the liquid side mass transfer coefficient measured for a pure solution of surfactants: it is significantly lower than those obtained with dilute solutions of surfactants, which is not surprising with regard to the higher viscosity and smaller surface tension of such solution (Table 2).

The associated diffusion coefficients of oxygen are calculated by using the k_L values previously determined and Eq. (14) with:

- $C_2 = 2.22.10^{-4}\,\mathrm{m.s^{-1}}$ for aqueous solutions of surfactants (as their viscosity and density are close to those of water, see Table 2),

- $C_2 = 2.22.10^{-4}\left(\frac{\rho_{L\ aqueous}}{\rho_{L\ pure}}\right)^{0.5} = 2.16.10^{-4}\ \mathrm{m.s^{-1}}$ for a pure solution of surfactants.

In Figure 6 are compared the experimental diffusion coefficients of oxygen at various surfactant concentrations with those in a pure solution of surfactants. A behavior similar to k_L (Figure 5) is observed: the diffusion coefficient of oxygen, *D*, decreases with an increase of surfactant concentration until the *CMC* is reached (1.9 $\mathrm{g.L^{-1}}$) and, for higher surfactant concentrations, *D* remains constant. Moreover, Figure 6 reveals that the diffusion coefficient of oxygen obtained in a pure solution of surfactant has the same order of magnitude than those measured above the *CMC* value ($5.45.10^{-10}$ against $6.96.10^{-10}$ $\mathrm{m^2.s^{-1}}$ respectively). This result would confirm that the low k_L values observed at high surfactant concentrations (Figure 5) are directly linked to the presence of surfactants which makes the diffusion coefficients of oxygen be reduced.

To better shed light on the effect of surfactants on liquid side mass transfer coefficient, two different hydrodynamic conditions are compared: a free gas-liquid interface sheared by a gas flow (here) and gas-liquid interfaces formed by a chain of bubbles having diameters above to 3.5 mm [1-2]. Figure 7 reports the associated results in terms of k_L at various surfactant concentrations. Firstly, as commonly observed in literature, the k_L values obtained in water are higher for the bubbling condition than those for the free interface condition; this is directly correlated to the levels of turbulence (and thus the Reynolds numbers) which are different in both cases (this effect is usually taken into account in the classical relationships linking the Sherwood number to the Reynolds and Schmidt numbers). In a second time, a quasi-linear relation between both hydrodynamics conditions appears in the whole range of surfactant concentrations. This involves thus that, whatever the hydrodynamic conditions, the effect of surfactants on liquid side mass transfer coefficient is similar. As, at a free interface, the decrease of k_L in presence of surfactants is linked to a change in diffusion

mechanism, Figure 7 suggests that an identical influence occurs in the case of the bubbling condition tested by [1]. These findings would thus demonstrate that, for bubbles having size above 3.5 mm, the effect of surfactants on k_L is mainly correlated to a variation in diffusion coefficients at the interface. Such a conclusion implies that:

- the true diffusion coefficient D (i.e. the one established in presence of surfactants) has to be introduced in the Schmidt number when the $Sh = f(Re,Sc)$ relations are used;
- as proposed by [2] for bubble sizes between 1 and 3.5 mm, the impact of surfactants has to be considered both on local hydrodynamics and diffusion coefficient.

4. Conclusions

Specific experiments were proposed to investigate the effect of surfactants on liquid side mass transfer coefficient. They were based on the determination, under controlled temperature and hydrodynamic conditions, of the liquid side mass transfer coefficient k_L at a free gas-liquid interface.

In a first step, the liquid side mass transfer coefficients k_L were measured in water at various temperatures and the associated diffusion coefficient of oxygen D were calculated. The effect of temperature observed experimentally was well correlated by the predictions issued from the Wilke-Chang, Scheibel and Hayduk-Laudie correlations. Coupled with additional experiments where the influence of the rotation speeds was tested, these data enabled the approach implemented to be validated.

Secondly, this methodology was applied in presence of surfactants identical to those used by [1-2]. A pure solution and various aqueous solutions of surfactants (concentrations ranging between 0.05 and 10 $g.L^{-1}$) were tested. A decrease of the liquid side mass transfer

coefficient with an increase of surfactant concentrations was observed as well as a plateau when the *CMC* was reached (i.e., $s_e = 1$); the smallest value was obtained for a pure solution of surfactant. The same behavior existed when the diffusion coefficient of oxygen was plotted as a function of surfactant concentration. Above the *CMC*, the equivalent diffusion coefficients had the same order of magnitude than the one measured in a pure solution of surfactant. These results confirmed that the low k_L values observed at high surfactant concentrations were directly linked to diffusion coefficients reduced by the presence of surfactants in the liquid film layer.

At last, the present results were compared with those obtained by [1-2] at gas-liquid interfaces formed by a chain of bubbles having diameters above to 3.5 mm. A quasi-linear relation between the k_L measured in both hydrodynamic conditions was revealed in the whole range of surfactant concentrations. This would indicate that, for both conditions of free interface and of bubbling at d_B>3.5 mm, the effect of surfactants on k_L was mainly correlated with a variation in diffusion coefficients at the interface.

References

[1] P. Painmanakul, K. Loubière, G. Hébrard, M. Mietton-Peuchot, M. Roustan, Effect of surfactants on liquid-side mass transfer coefficients, Chemical Engineering Science 60 (2005) 6480-6491.

[2] R. Sardeing, P. Painmanakul, G. Hébrard, Effect of surfactants on liquid-side mass transfer coefficients in gas-liquid systems: A first step to modelling, Chemical Engineering Science 61 (2006) 6249-6260.

[3] S.S. Alves, S.P. Orvalho, J.M.T. Vasconcelos, Effect of bubble contamination on rise velocity and mass transfer, Chemical Engineering Science 60 (2005) 1-9.

[4] V. Linek, T. Moucha, M. Kordac, Mechanism of mass transfer from bubbles in dispersions Part I. Danckwerts' plot method with sulphite solutions in the presence of viscosity and surface changing agents, Chemical Engineering and Processing 44 (2005) 353-361.

[5] V. Linek, T. Moucha, M Kordac, Mechanism of mass transfer from bubbles in dispersions Part II. Mass transfer coefficients in stirred gas-liquid reactor and bubble column, Chemical Engineering and Processing 44 (2005) 121-130.

[6] D. Rosso, D.L. Huo, M.K. Stenstrom, Effects of interfacial surfactant contamination on bubble gas transfer, Chemical Engineering Science 61 (2006) 5500-5514.

[7] J.M.T Vasconcelos, J.M.L. Rodrigues, S.C.P. Orvalho, S.S. Alves, R.L. Mendes, A. Reis, Effect of contaminants on mass transfer coefficients in bubble column and airlift contactors, Chemical Engineering Science 58 (2003) 1431-1440.

[8] G. Vazquez, M.A. Cancela, C. Riverol, E. Alvarez, J.M. Navaza, Application of the Danckwerts method in a bubble column: effect of surfactants on mass transfer coefficient and interfacial area, Chemical Engineering Journal 78 (2000) 13-19.

[9] B. Cuenot, J. Magnaudet, B. Spennato, The effects of slightly soluble surfactants on the flow around a spherical bubble, Journal of Fluid Mechanics 399 (1997) 25–53.

[10] A. Dani, A. Cockx, P. Guiraud, Direct numerical simulation of mass transfer from spherical bubbles: the effect of interface contamination at low Reynolds numbers, International Journal of Chemical Reactor Engineering 4 (2006) A2.

[11] K. Loubière, G. Hébrard, Influence of surface tension (surfactants) on the bubble formation at rigid and flexible orifices, Chemical Engineering and Processing 43 (2004) 1361-1369

[12] M. Roustan, Transferts gaz-liquide dans les procédés de traitement des eaux et des effluents gazeux, Editions Dec & Doc (2003). Paris

[13] P.V. Danckwerts, Significance of liquid film coefficients in gas absorption, Ind. Eng. Chem. 43 (1951) 1460-1467.

[14] G.E. Fortescue, J.R.A Pearson, On gas absorption in a turbulent liquid, Chemical Engineering Science 22 (1967) 9 1163-1176.

[15] S. Banerjee, Turbulence-interface interactions, Phase-Interface Phenomena in Multiphase Flow (1991) Hemisphere Publishing Corporation

[16] A. Cockx, M. Roustan, A. Liné, G. Hébrard, Modelling of mass transfer coefficient k_L in bubble columns, Trans IChemE 73 (1995) A 627-631.

[17] R.H. Perry, D.W. Green, Perry's chemical engineer's handbook, 7th edition McGraw-Hill (1997) New-York

[18] C.O. Bennett, I.J.E., Momentum, heat and mass transfer, 2nd edition McGraw-Hill Chemical Engineering Series (1967)

[19] J.E. Vivian, C.J. King, The mechanism of liquid-phase resistance to gas-absorption in a packed column, AIChE Journal (1964) 10:221-227

[20] C.R Wilke, P. Chang, Correlation of diffusion coefficients in dilute solutions, AIChE Journal 1 (1955) 2 264-270.

[21] R.C. Reid, J.M. Praunsnitz, T.K. Sherwood, The Properties of Gases and Liquids, 3rd Edition McGraw-Hill (1977) New-York 578.

[22] E.G Scheibel, Physical chemistry in chemical engineering design, Ind. Eng. Chem. (1954) 46

[23] W. Hayduk, H. Laudie, Prediction of diffusion-coefficients for nonelectrolytes in dilute aqueous solutions, AIChE J. (1974) 20(3):611-615

[24] K.A. Reddy, L.K. Doraiswamy, Estimating liquid diffusivity, Ind. Eng. Chem. Fundam. (1967) 6:77-79

[25] M.A. Lusis, G.A. Racliff, Diffusion in binary liquid mixtures at infinite dilution, Can. J. Chem. Eng. (1968) 46(5):385-386

[26] M.T. Tyn, W.F. Calus, Temperature and concentration-dependence of mutual diffusion-coefficients of some binary-liquid systems, J. Chem. Eng. Data (1975) 20(3):310-316

[27] N.O. Umesi, R.P. Danner, Predicting diffusion-coefficients in non-polar solvents, Ind. Eng. Chem. Process Des. Dev. (1981) 20(4):662-665

[28] M.A. Siddiqi, K. Lucas, Correlations for prediction of diffusion in liquids, Can. J. Chem. Eng. (1986) 64(5):839-843

[29] N.B. Bird, W.E. Stewart, E.N.Lighfoot, Transport Phenomena, John Wiley (1960)

Notation

a	Interfacial area	$[L^{-1}]$
C	Dissolved oxygen concentration in the liquid phase	$[mol.L^{-3}]$
C^*	Dissolved oxygen concentration at saturation in the liquid phase	$[mol.L^{-3}]$
C_O	Dissolved oxygen concentration in the liquid phase at initial time	$[mol.L^{-3}]$
D	Diffusion coefficient of oxygen in the liquid phase under test	$[L^2.T^{-1}]$
D_{AB}^0	Diffusion coefficient of the solute A into the solvent B in the case of a binary and infinite diluation	$[L^2.T^{-1}]$
k_La	Volumetric mass transfer coefficient	$[T^{-1}]$
k_L	Liquid side mass transfer coefficient	$[L.T^{-1}]$
N	Rotation speed of the magnetic agitator	$[T^{-1}]$
s'	Renewal rate of liquid elements at the gas-liquid interface	$[T^{-1}]$
s_e	Surface cover ratio	[-]

S	Signal emitted by the oxygen micro-probe	[-]
S^*	Signal emitted by the oxygen micro-probe at saturation	[-]
S_0	Signal emitted by the oxygen probe at the initial time	[-]
U_G	Gas velocity	$[L.T^{-1}]$
U_i^*	Interfacial momentum transfer velocity	$[L.T^{-1}]$
U_L	Liquid velocity	$[L.T^{-1}]$
t	Time	$[T^{-1}]$
T	Temperature	[K]

Greek letters

α	Oxygen solubility	$[mol.M^{-3}]$
τ_i	Interfacial momentum transfer stress	$[M.L^{-1}.T^{-2}]$
μ	Viscosity	$[M.L^{-3}]$
ρ	Density	$[M.L^{-3}]$

Dimensionless number

Sc	Schmidt number $Sc = \frac{\mu_L}{\rho_L D}$	[-]

Index

G	Gas phase
L	Liquid phase
W	Water

Figure legend

Figure 1: Schematic representation of the experimental set-up: (1) Double wall vessel, (2) Oxygen micro-probe Unisense®, (3) Acquisition system, (4) Thermometer,

(5) Thermo-regulation, (6) Magnetic agitator, (7) Gas flowmeter, (8) Nitrogen supply, (9) Air supply, (10) Three-way valve

Figure 2: Typical response curve obtained with the oxygen micro-probe

Figure 3: Graphical determination of the volumetric mass transfer coefficient $k_L a$

Figure 4: Comparison between the diffusion coefficients of oxygen in water measured and those estimated by empirical correlations (Eqs. 16-18) at various temperatures (N = 100 rpm). The molar volume of oxygen at its normal boiling point (in $cm^3.mol^{-1}$) is put in brackets.

Figure 5: Liquid side mass transfer coefficient versus surfactant concentration (N = 100 rpm, T = 20°C): experimental data for different concentrations (●) and for a pure solution of surfactant (--).

Figure 6: Diffusion coefficient of oxygen versus surfactant concentration (N = 100 rpm, T = 20°C): experimental data for different concentrations (●) and for a pure solution of surfactant (— —)

Figure 7: Relation between the liquid side mass transfer coefficients obtained for a chain of bubbles and for a free gas-liquid interface (at 20°C and at various surfactant concentrations)

Table legend

Table 1: Experiments in water at various temperatures: density (ρ_W), dynamic viscosity (μ_W), volumetric mass transfer coefficient ($k_L a$) and liquid mass coefficient (k_L) (N = 100 rpm)

Table 2: Properties of the aqueous and pure solutions of surfactants (T = 20°C)

Table 3. Experiments in water at various rotation speeds (T = 20°C): liquid mass coefficient k_L and constant C_2

Table 1. Experiments in water at various temperatures: density (ρ_W), dynamic viscosity (μ_W), volumetric mass transfer coefficient ($k_L a$) and liquid mass coefficient (k_L) (N = 100 rpm)

T (°C)	ρ_W (kg.m^{-3})	μ_W (cP)	$k_L a$ (s^{-1})	k_L (m.s^{-1})
5	999.96	1.52	$1.80.10^{-4}$	$6.30.10^{-6}$
20	998.20	1.00	$2.83.10^{-4}$	$9.91.10^{-6}$
35	994.03	0.70	$4.06.10^{-4}$	$1.42.10^{-5}$
50	998.04	0.55	$5.31.10^{-4}$	$1.86.10^{-5}$

Table 2. Properties of the aqueous and pure solutions of surfactant (T = 20°C)

Surfactant concentration ($g.L^{-1}$)	ρ_L ($kg.m^{-3}$)	μ_L (cP)	σ_L ($mN.m^{-1}$)	s_e (-)
0.05	998.2	1.00	69.78	0.4
0.2			60.45	0.8
1.9			39.70	1
10			39.70	1
Pure solution of surfactant	1050.0	35.00	33.00	-

Table 3. Experiments in water at various rotation speeds (T = 20°C): liquid mass coefficient k_L and constant C_2

N (rpm)	k_L (m.s^{-1})	C_2
50	$1.02.10^{-5} \pm 0.1.10^{-5}$	$2.27.10^{-4} \pm 0.23.10^{-4}$
100	$9.91.10^{-6} \pm 0.95.10^{-6}$	$2.22.10^{-4} \pm 0.21.10^{-4}$
120	$9.35.10^{-5} \pm 0.84.10^{-5}$	$2.09.10^{-4} \pm 0.21.10^{-4}$

Fig. 1. Schematic representation of the experimental set-up: (1) Double wall vessel, (2) Oxygen micro-probe Unisense®, (3) Acquisition system, (4) Thermometer, (5) Thermo-regulation, (6) Magnetic agitator, (7) Gas flowmeter, (8) Nitrogen bottle, (9) Air bottle, (10) Three-way valve

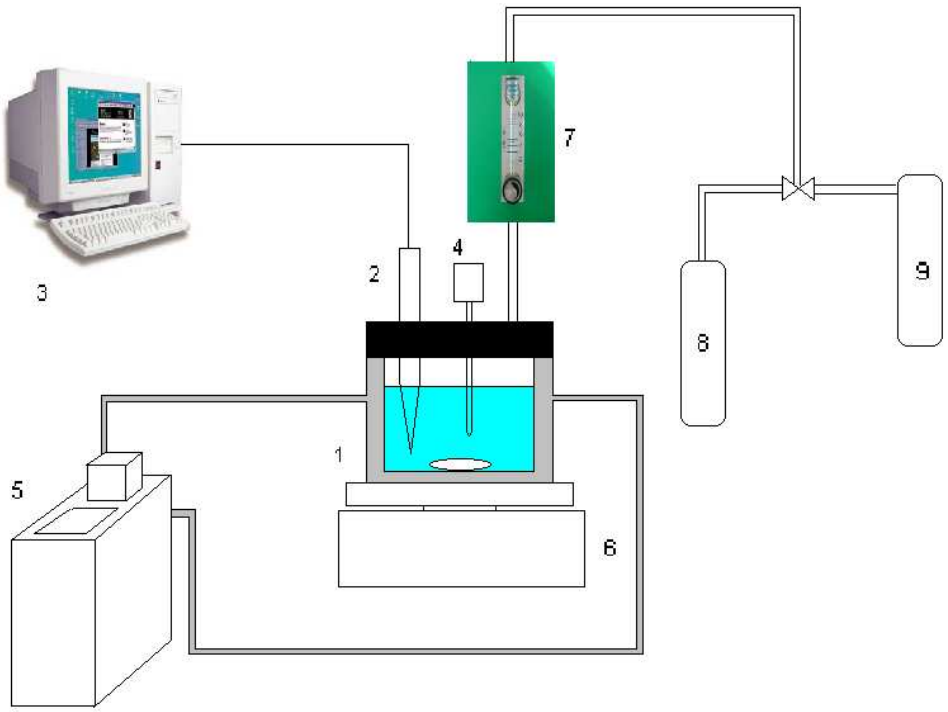

Fig.2. Typical response curve obtained with the oxygen micro-probe

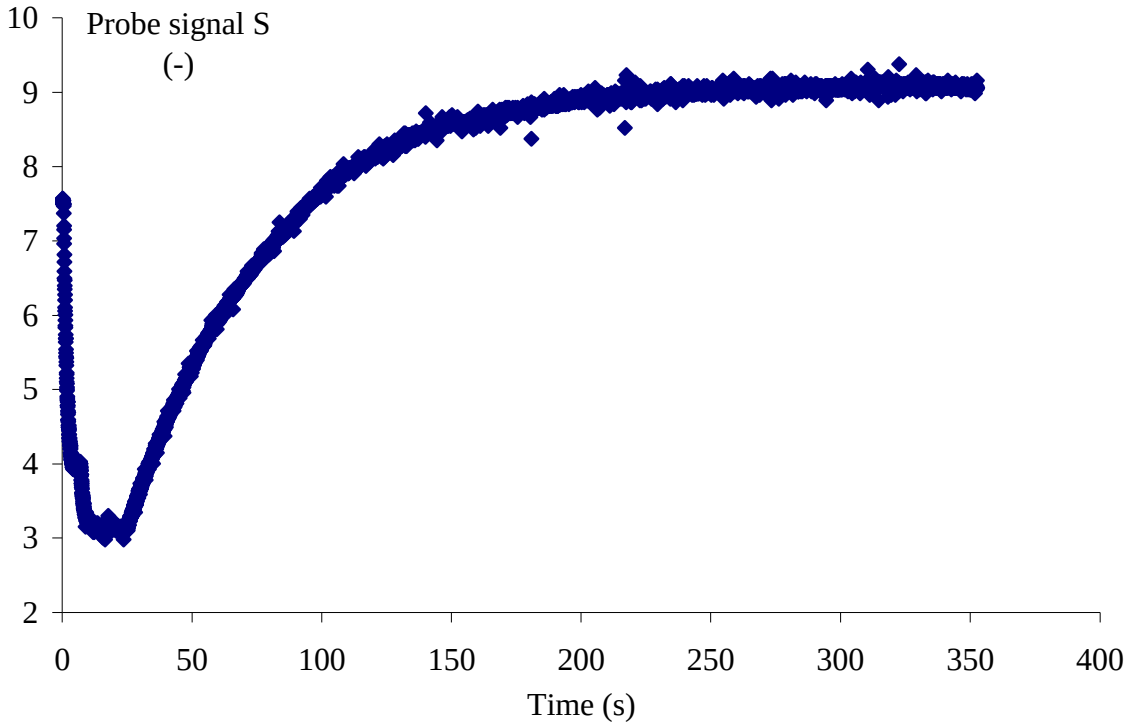

Fig. 3. Graphical determination of the volumetric mass transfer coefficient $k_L a$

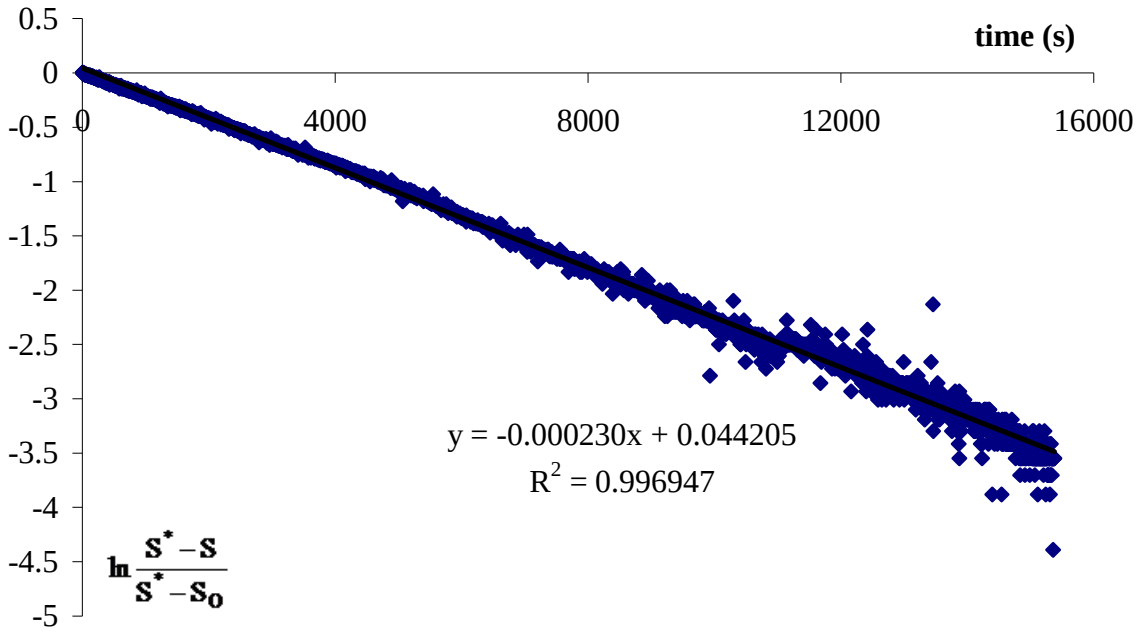

Fig. 4. Comparison between the diffusion coefficients of oxygen in water measured and those estimated by empirical correlations (Eqs. 16-18) at various temperatures (N = 100 rpm). The molar volume of oxygen at its normal boiling point (in $cm^3.mol^{-1}$) is put in brackets.

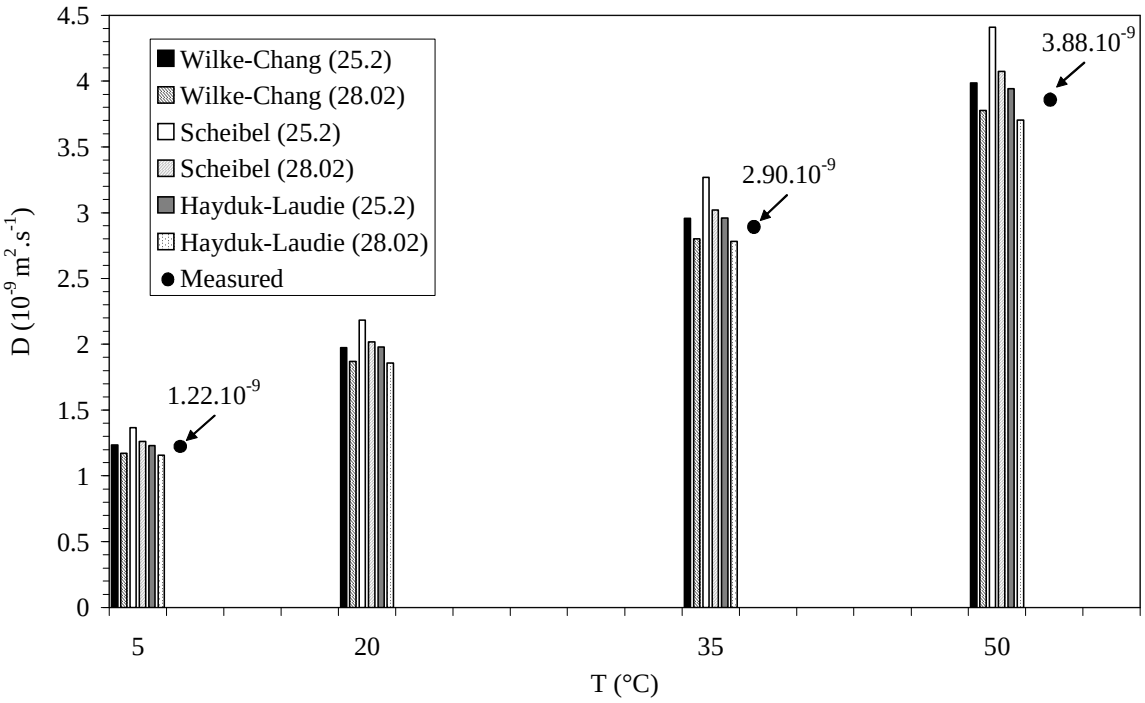

Fig. 5. Liquid side mass transfer coefficient versus surfactant concentration (N = 100 rpm, T = 20°C): experimental data for different concentrations (●) and for a pure solution of surfactant (--)

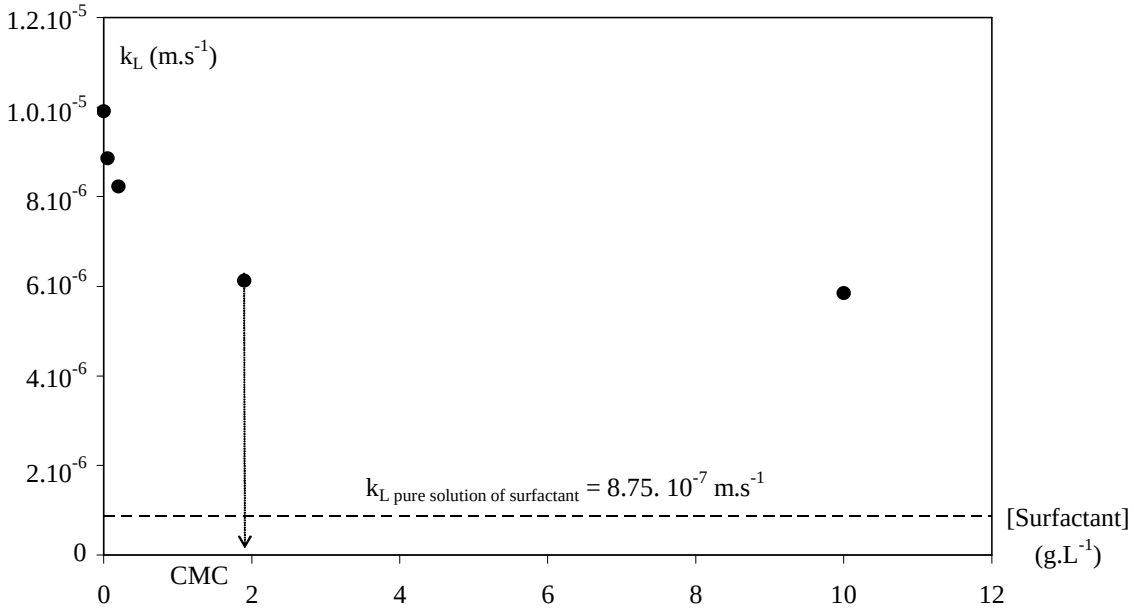

Fig. 6. Diffusion coefficient of oxygen versus surfactant concentration (N = 100 rpm, T = 20°C): experimental data for different concentrations (●) and for a pure solution of surfactant (– –)

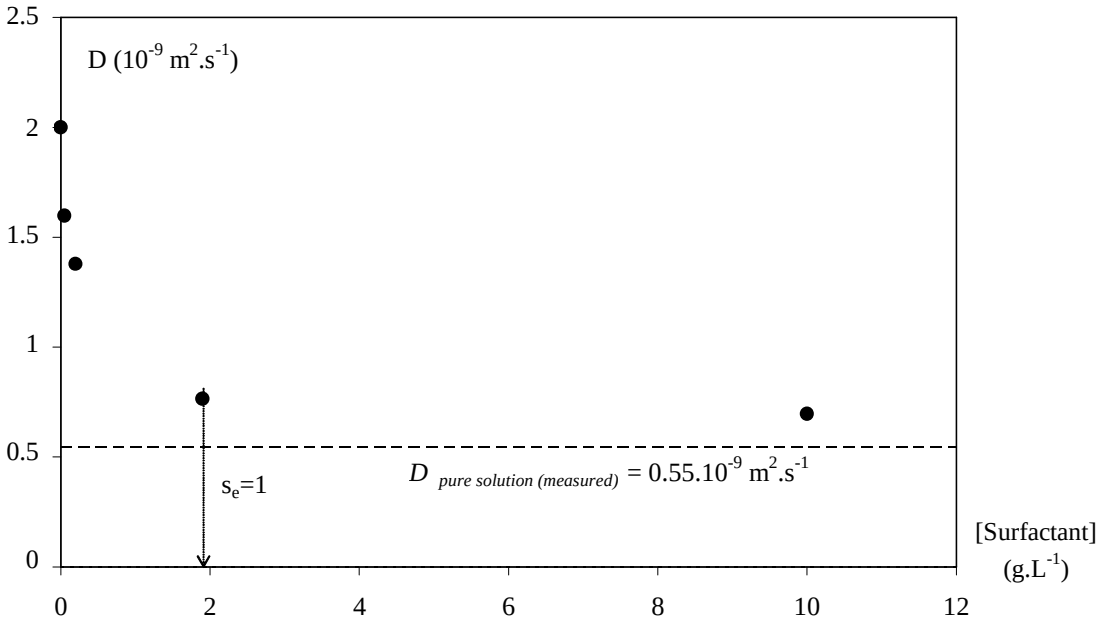

Fig. 7. Relation between the liquid side mass transfer coefficients obtained for a chain of bubbles and for a free gas-liquid interface (at 20°C and at various surfactant concentrations)